ROYAL SOCIETY OPEN SCIENCE

royalsocietypublishing.org/journal/rsos

Research

Cite this article: Le Moal A, Payton L, Tran D, Daramy F, Botté A, Pogoda B, Meyer B. 2025 Identification and expression of circadian clock genes in the European flat oyster *Ostrea edulis*. *R. Soc. Open Sci.* **12**: 250970. https://doi.org/10.1098/rsos.250970

Received: 21 May 2025
Accepted: 7 November 2025

Subject Category:
Organismal and evolutionary biology

Subject Areas:
behaviour, molecular biology, environmental science

Keywords:
circadian clock, *Ostrea edulis*, biological rhythm, bivalve, phylogenetic tree, gene expression, valve behaviour

Authors for correspondence:
Alexandre Le Moal
e-mail: alexandre.lemoal@awi.de
Bettina Meyer
e-mail: Bettina.Meyer@awi.de

Supplementary material is available online at https://doi.org/10.6084/m9.figshare.c.8154231.

THE ROYAL SOCIETY PUBLISHING

Identification and expression of circadian clock genes in the European flat oyster *Ostrea edulis*

Alexandre Le Moal[1,2], Laura Payton[4,5], Damien Tran[4,5], Flore Daramy[4], Audrey Botté[4], Bernadette Pogoda[3] and Bettina Meyer[1,2,6]

[1]Institute for Chemistry and Biology of the Marine Environment, Carl von Ossietzky University of Oldenburg, Oldenburg, Germany
[2]Section Polar Biological Oceanography, and [3]Section Shelf Seas Systems Ecology, Alfred Wegener Institute, Helmholtz Centre for Polar and Marine Research, Bremerhaven, Germany
[4]Univ. Bordeaux, CNRS, Bordeaux INP, EPOC, UMR 5805, Arcachon, France
[5]GDR2202 – Lumière & environnement nocturne (LUMEN), UMR 5602 GÉODE, CNRS, University of Toulouse – Jean Jaurès, Toulouse, France
[6]Helmholtz Institute for Functional Marine Biodiversity at the University of Oldenburg (HIFMB), Oldenburg, Germany

ALM, 0009-0000-2550-4473; LP, 0000-0001-5090-0929; DT, 0000-0002-7432-7765; FD, 0000-0002-1141-4554; BP, 0000-0003-3997-426X; BM, 0000-0001-6804-9896

Circadian clocks enable organisms to synchronize their biological processes to environmental daily cycles, thereby increasing species fitness. Components of the molecular clock are conserved across many taxa, though their structure and function can vary. In this study, we aim to investigate the circadian clock of the European flat oyster *Ostrea edulis*, an endangered species with a pivotal role in biogenic reef ecosystems. Phylogenetic and protein domain analyses were performed to identify orthologues of core clock and clock-associated genes (*OeClock*, *OeBmal1*, *OePeriod*, *OeTimeless*, *OeCryptochrome2*, *OeRev-erb*, *OeRor*, *OeDoubletime*, *OeClockWorkOrange*, *OeShaggy*), a gene related to melatonin synthesis (*OeHiomt*) and genes involved in light perception (*OeCryptochrome1*, *OeOpsin4*). As a functional output of the clock, we observed daily and circadian rhythms in valve behaviour recorded under light:dark and constant dark conditions. In parallel, gene expression analyses in two tissues under similar light regimes revealed tissue-specific rhythms, suggesting the presence of a functional and plastic endogenous circadian system in *O. edulis*. These findings offer a first molecular work for deeper exploration of the circadian clock functioning in *O. edulis*, providing essential resources to investigate its evolutionary adaptation to cyclic environments, and inform restoration and conservation strategies of this threatened species.

1. Introduction

Life on Earth has been confronted with environmental cycles of varying periods, influenced by the interactions between the Sun, the Earth and Moon trajectories [1]. In order to adapt and survive in these dynamic environments, organisms have developed an endogenous timing mechanism. This internal clock enables organisms to synchronize with their environment and anticipate daily environmental fluctuations, thereby regulating various metabolic, physiological and behavioural processes [2]. Research across various taxa, including vertebrates [3], insects [4,5] and crustaceans [6], reveals that while the molecular architecture of circadian clocks may differ, fundamental clock genes are mostly conserved, although their functions and interactions may vary across phyla [7]. The molecular mechanisms of a circadian clock involves negative and positive transcriptional and translational feedback loop interactions among clock genes and their proteins [8–10]. This molecular system maintains a circadian rhythm (literally *about a day*) even without external stimuli, i.e. under free-running conditions [11]. To stay in synchronization with external cycles, the clock is entrained by environmental cues called *zeitgebers* (time givers) [4]. The daily light/dark cycle is the primary *zeitgeber* for the circadian clock, as it is the most reliable environmental cue for daily cycles [12,13]. Marine organisms exist in a complex environment influenced not only by the daily light/dark cycle but also by cycles of shorter or longer durations, such as tidal, lunar/semi-lunar or seasonal cycles [14,15]. The functional mechanisms of molecular clocks in marine invertebrates remain poorly characterized. In bivalves, studies on species such as the Pacific oyster *Crassostrea gigas* [16,17], the blue mussel *Mytilus edulis* [18] and the Arctic scallop *Chlamys islandica* [19] show the presence of orthologues of core and related circadian clock genes, indicating a high degree of conservation.

The European native oyster, *O. edulis*, was formerly found throughout Europe, from intertidal coastal areas to deeper offshore waters [20–22]. Today, this ecological key species is under severe threat due to overfishing, habitat degradation, habitat loss, pollution and invasive diseases (e.g. *Marteilia*, *Bonamia*) [23]. Native oysters are highly gregarious, meaning that oyster larvae prefer to settle where other oysters are present, allowing them to form a structured biogenic reef habitat for different species [24]. Native oyster habitats, known as oyster reefs, provide key ecosystem functions and enhance biodiversity [25]. Therefore, the conservation of European flat oyster populations has recently become a focus of ecological restoration efforts [26]. Despite the ecological importance of *O. edulis*, little is known about the environmental drivers of its biological rhythms, which limits the understanding of its resilience to climate-induced environmental changes and, consequently, its conservation efforts. A recent study highlighted that this oyster exhibits a daily rhythm of valve behaviour synchronized by light/dark cycles, that persists under constant darkness [27]. These findings demonstrate the presence of a functional endogenous clock mechanism that is highly synchronizable by light. However, to date, the molecular clock components and circadian clockwork of *O. edulis* have yet to be investigated. While mollusc and bivalve genome sequencing and assembly have traditionally been hindered by technical and genetic complexities, as these organisms often possess large, highly repetitive and heterozygous genomes [28,29], a recent study has integrated multiple technologies to produce a high-quality chromosome-level reference genome for the European flat oyster, paving the way to explore its molecular circadian clockwork [30].

The present study focuses on identifying the circadian clock genes responsible for generating and synchronizing rhythms in *O. edulis*. The objective of the study is to identify 13 orthologous genes that are putatively involved in the clock machinery, including 10 circadian clock genes (*OeClock*, *OeBmal1*, *OePer1*, *OeTim1*, *OeCry2*, *OeRev-erb*, *OeRor*, *OeDbt*, *OeCwo*, *OeShag*), 1 gene involved in melatonin synthesis (*OeHiomt*), and 2 photoreceptor genes (*OeCryptochrome1*, *OeOpn4*). Furthermore, the gene expression patterns in gills and labial palps are investigated under light/dark cycles and constant darkness. Concurrently, we monitor and analyse the daily and circadian rhythms of valve behaviour, which are an output of the circadian clockwork. Based on these analyses, we hypothesize that *O. edulis* possesses a functional endogenous circadian system, exhibiting tissue-specific gene expression patterns and synchronizing behavioural rhythms. Therefore, the goal of this study is first to characterize the molecular components of the circadian clock in *O. edulis*, and second to explore their potential involvement in generating behavioural rhythms, providing preliminary insight into the temporal organization of biological rhythms in this ecologically important and threatened species.

2. Material and methods

2.1. Clock gene mining

A bioinformatic analysis was conducted to identify genes of interest involved or related to the circadian clock machinery. Gene mining was performed using the National Center for Biotechnology Information (NCBI) database (https://www.ncbi.nlm.nih.gov/) along with the reference genome assembly xbOstEdul1.1 (NCBI RefSeq assembly GCF_947568905.1 [30]). For genes that were already predicted and annotated (*OeClock*, *OeBmal1*, *OeTimless* (*OeTim1*), *OeRor*, *OeDoubletime* (*OeDbt*), *OeShaggy* (*OeShag*), *OeCryptochrome1* (*OeCry1*) and *OeOpsin4* (*OeOpn4*)), a protein–protein BLAST (blastp) was performed based on corresponding proteins described in other species, and the corresponding protein sequences were downloaded in FASTA format for further analysis and validation. For non-annotated genes (*OePeriod* (*OePer1*), *OeCryptochrome2* (*OeCry2*), *OeRev-erb*, *OeClockWorkOrange* (*OeCwo*), and *OeHiomt*), a protein–protein BLAST (blastp) was conducted based on corresponding proteins described in other species. Blastp searches were filtered with a value of $E < 1 \times 10^{-5}$. Sequences with >30% identity were retained, or >25% in rare cases when conserved domains were confirmed. Partial, likely non-functional or misannotated sequences were excluded based on sequence integrity and domain structure. To ensure that the identified sequences correspond to the genes of interest, once all genes were identified, the sequences were analysed using InterProScan (https://www.ebi.ac.uk/interpro/) to investigate specific protein domains and validate their relevance to the clock mechanism under investigation. Accession numbers for identified genes are available in electronic supplementary material, table S1.

2.2. Phylogenetic tree construction and representation

DNA sequences were aligned using the MUSCLE method implemented in MEGA X (https://www.megasoftware.net/). To enhance alignment quality, Gblocks (http://phylogeny.lirmm.fr/phylo_cgi/) was employed to trim the alignment, ensuring the removal of poorly aligned positions and divergent regions. Phylogenetic trees were constructed in MEGA X based on a consensus sequence common to all analysed species, incorporating the protein domains of interest. Model selection for each tree was performed using the maximum likelihood (ML) approach within MEGA X, prioritizing models with the highest Akaike information criterion (AIC) and log-likelihood (lnL) scores. Once the optimal model was identified, trees were generated in MEGA X using the ML method based on the Jones–Taylor–Thornton matrix model with 1000 bootstrap replicates to assess statistical support and were represented using FigTree software (http://tree.bio.ed.ac.uk/software/figtree/). Two phylogenetic trees were constructed for each gene. The first one includes multiple phyla of the animal kingdom and the second one is at the bivalve level. Phylogenetic trees were constructed only when enough sequences from other species were available. To ensure broad representation across families, we selected the maximum number of clearly annotated or identified bivalve sequences available in public databases. For Animalia-level trees, representative bivalves were included alongside sequences from other major metazoan lineages, but a limited number of bivalve sequences was retained to avoid overrepresentation and maintain balanced comparisons across phyla. Accession numbers of genes used to construct phylogenetic trees are provides in electronic supplementary material, table S1 for *Ostrea edulis* sequences and dataset S1 for other species.

2.3. Experimental model

All research conducted in this study adhered to French legislation and followed international ethical standards. The experiments were performed at the Marine Station of Arcachon, France, involving a total of 240 native European oysters (*O. edulis*). The oysters were sourced from a single farm located in Loch Ryan, southwest Scotland (coordinates: 54° 59′ 10″ N, 5° 03′ 18″ W), cultivated in subtidal conditions (Rossmore Oysters Ltd). Before the experiment, the oysters (approximately 8–10 years old; average shell length: 74.8 mm; average shell width: 72.5 mm) were acclimatized for one month in a continuous system utilizing natural seawater from Arcachon Bay. During this acclimatization period, microalgae (*Chaetoceros calcitrans*) were continuously incorporated into their diet, and the oysters were maintained under natural light conditions with no tidal cycle.

2.4. Experimental setup

Investigations into circadian behaviours and the expression of clock genes were conducted in two 17-day experiments at the Marine Station of Arcachon during winter 2022: the light:dark (L:D) experiment took place from 12 November to 29 November 2022, while the constant darkness (D:D) experiment ran from 5 December to 21 December 2022 (figure 1). Experiments were performed in winter to minimize confounding effects of reproductive cycles or sex change in *O. edulis* on the measured molecular and behavioural rhythms. In each experiment, 120 oysters were divided into two groups of 60 oysters each, with each group placed in distinct experimental units (EU1 and EU2) measuring 74.8 × 54.8 × 40.8 mm^3. The seawater in each unit was continuously supplied with oxygenated and filtered seawater (filter diameter < 1 μm) from Arcachon Bay at a flow rate of 350 ml min^{-1} per EU, maintaining a constant mean temperature of 15 ± 0.1°C, a pH of 7.9 ± 0.1 and a salinity of 33.1 ± 0.1‰. Prior to the start of the experiment, the oysters were acclimated to the experimental setup for 4 days. Each experiment began with a 7-day pre-exposure phase under a 12 h light:12 h dark cycle (L:D), followed by a 10-day L:D exposure phase corresponding to the same 12 h light:12 h dark cycle for the L:D experiment and a 10-day constant darkness (D:D) phase for the D:D experiment (figure 1).

The L:D conditions were achieved using white LED light bars (model MH3SP3 DSunY, 413–685 nm, peak at 553 nm), positioned above each EU. Photophase occurred from 07.00 to 19.00 (all times noted in local time, UTC+1), with the light intensity varying gradually to mimic the natural light cycle, reaching a maximum light intensity of 1406.1 ± 136.2 lx (mean ± standard error), corresponding to 28.99 μE m^{-2} s^{-1} in measured irradiance, between 12.30 and 13.30. Illuminances were measured underwater in each EU at the oysters' depth in lx using a handheld spectroradiometer (Blue-Wave UVN-100, StellarNet Inc.). Equivalent irradiance in μE m^{-2} s^{-1} was also measured using a portable radiometer (MICRO Class, Profiling (in-water), E (irradiance) PAR sensor, Biospherical Instrument Inc.). In chronobiological studies, time is expressed as zeitgeber time (ZT) during light/dark (LD) conditions, where ZT0 corresponds to the onset of the light phase (lights-on), and as circadian time (CT) under constant conditions such as dark/dark (DD), with CT0 aligned to subjective lights-on based on the preceding LD cycle. Thus, in our study, ZT/CT0 corresponds to 07.00, ZT/CT12 to 19.00, and maximal light intensity occurs at ZT6.

2.5. *Ostrea edulis* valve behaviour measurement

For each experiment, the valve activity of 24 oysters (12 per EU) was measured using high-frequency non-invasive (HFNI) valvometers. The measurement system consists of a pair of lightweight electrodes (each weighing < 100 mg) affixed to each half-shell of the oyster to minimize behavioural disturbance. Each electrode is connected via a flexible cable to the HFNI valvometer, allowing unrestricted movement of the oysters. An electromagnetic current generated between the electrodes enables the measurement of valve activity every 4.8 s. Additional details regarding the methodology can be found in Tran *et al*. [31] and Le Moal *et al*. [32]. Raw daily recordings were processed using LabVIEW 8.0 software (National Instruments, Austin, TX, USA). The valve opening amplitude (VOA) was recorded. The individual hourly VOA for each oyster was analysed as a percentage, where 100% indicates maximum valve opening amplitude throughout the hour and 0% indicates complete closure. Intermediate values represent varying degrees of opening amplitude. The mean hourly VOAs are represented as double-plotted actograms, where each line represents 2 days (figure 2). In an actogram, hourly activity levels above the daily median are represented by black bars, while hourly activity levels below the daily median are represented by light grey bars. Hourly individual VOA data are accessible in electronic supplementary material, dataset S2.

2.6. Time-series sampling for molecular investigation

The study of molecular rhythms was conducted using time-series sampling of gills and labial palps during both the L:D and D:D experiments. Sampling occurred on the second day of the exposure phase of each experiment, at 2 h intervals over a 24 h period across 13 time points (figure 1). For each

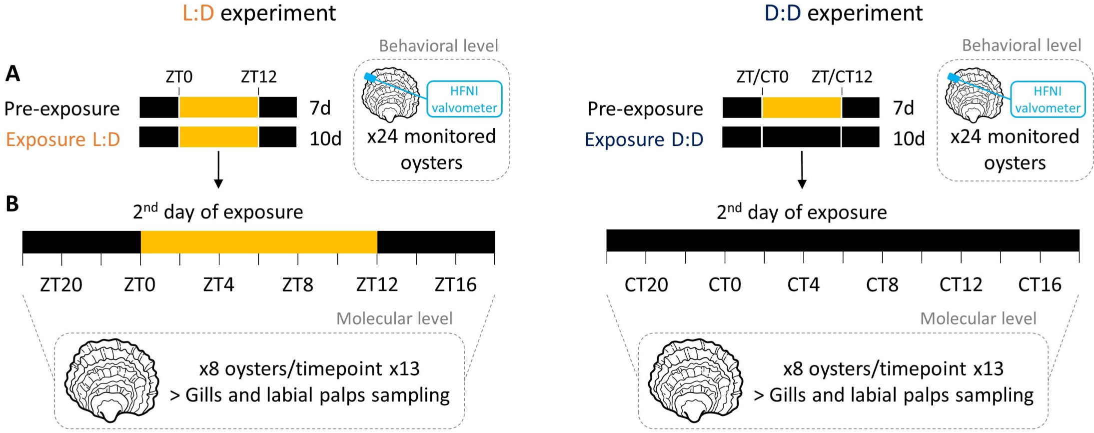

Figure 1. Experimental setup. (A) Experimental setup to investigate the rhythm of valve activity behaviour of *O. edulis* under L:D 12:12 and D:D. (B) Experimental protocol of time-series sampling for molecular investigation. Black bars = scotophase, yellow bars = photophase. ZT: *zeitgeber* time; CT: circadian time.

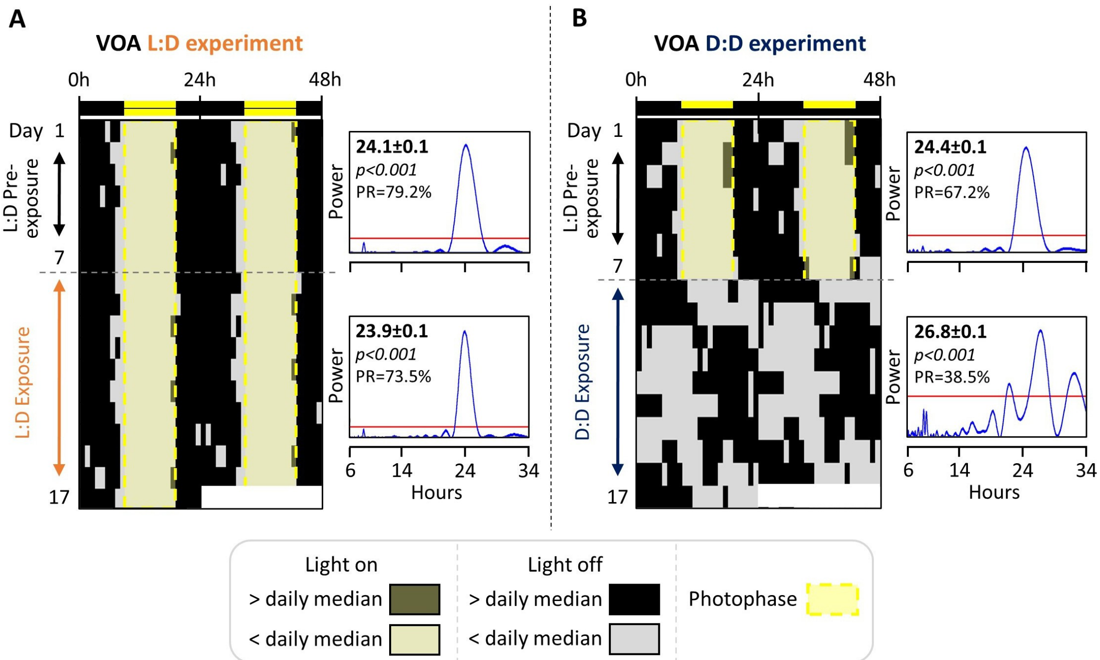

Figure 2. Actograms and chronobiological analyses of *O. edulis* valve activity. Actograms of mean valve opening amplitude (VOA; $n = 24$ individuals per experiment) during the 17 days of the L:D experiment (A) and during the 17 days of the D:D experiment (B). Each actogram represents the 7 days of pre-exposure and the 10 days of exposure for both experiments. For each pre-exposure and exposure phase, the Lomb and Scargle periodogram (LS) and characteristics of the Cosinor model are associated: the period (*h*) ± s.e. (indicated in bold), the *p*-value, and the percent rhythm (PR, %). The red line on the LS periodogram indicates a threshold of significance ($p = 0.95$). The rhythm is considered significant for the Cosinor model with $p < 0.05$. In the actograms, yellow areas indicate the photophase, and the dotted yellow lines represent the times when the light is turned on and off. The yellow and black bars at the top of the actograms depict the light and dark phases, respectively. Hourly individual VOA data are accessible in electronic supplementary material, dataset S2.

time point, 8 oysters were sampled in total (4 in EU1 and 4 in EU2). In the L:D experiment, samples were collected on 22–23 November (10.00–10.00), while in the D:D experiment, sampling took place on 13–14 December (10.00–10.00) (figure 1). All dissections conducted were performed under red light to minimize disturbance to the oysters. Gills and labial palp tissues were dissected and immediately immersed in RNA Later. Samples were then stored at 4°C for 24 h before being transferred to −80°C for long-term preservation prior to laboratory analysis.

2.7. Total RNA extraction and cDNA synthesis

Total RNA was extracted from gills using Trizol (Invitrogen) and a Direct-zol™ RNA MiniPrep (Zymo Research). The quantity and quality of total RNA were assessed by spectrophotometry (OD230, OD260, OD280). RNA reverse transcription was performed using RevertAid H Minus First Strand cDNA Synthesis Kits (Thermo Scientific).

2.8. mRNA expression analysis by real-time polymerase chain reaction

Primers for genes of interest (*OeClock*, *OeBmal1*, *OePer1*, *OeTim1*, *OeCry2*, *OeRev-erb*, *OeRor*, *OeDbt*, *OeCwo*, *OeShag*, *OeHiomt*, *OeCry1*, *OeOpn4*) as well as for housekeeping genes (*OeGapdh*, *OeEf1*, *Oe28S*) were designed using the coding sequences (CDS) of these genes, with the assistance of Primer3Plus (https://www.bioinformatics.nl/cgi-bin/primer3plus/primer3plus.cgi). Forward and reverse sequences for the primers are detailed in electronic supplementary material, table S1. Real-time quantitative PCR (qPCR) was performed with a PowerUp™ SYBR™ Green Master Mix kit (Fisher Scientific). The qPCR reactions were conducted under the following conditions: an initial activation step at 95°C for 2 min to activate the Dual-Lock™ DNA polymerase, followed by 40 cycles of denaturation at 95°C for 15 s, and annealing and extension at 60°C for 1 min to amplify the target cDNA. At the conclusion of amplification, melting curves were generated by gradually decreasing the temperature from 95°C to 60°C to verify primer specificity. Relative transcript levels of clock and clock-associated genes were determined using the comparative Ct method ($2^{-\Delta Ct}$) as described by Livak & Schmittgen [33], where ΔCt is calculated as $Ct_{(\text{target gene})} - Ct_{(\text{housekeeping gene})}$. Gene expression was normalized using the geometric mean of the housekeeping genes *OeEf1*, *OeGapdh* and *Oe28S*. The choice of these housekeeping genes was supported by previous studies validating their reliability for normalization in gene expression analyses [34,35]. Based on stability values [36] and MIQE guidelines [37], gene expression was normalized using the geometric mean of the housekeeping genes *OeEf1*, *OeGapdh* and *Oe28S*. The mean Ct values for these genes during L:D and D:D in gills and labial palps are reported in electronic supplementary material, figure S1. Electronic supplementary, dataset S3, provides detailed gene expression data in gills and labial palps during L:D and D:D experiments.

2.9. Chronobiological analyses

For the behavioural study, chronobiological analyses were conducted on hourly VOA datasets using the software Time Series Analysis Serial Cosinor 6.3. Several steps were necessary to validate a significant rhythm. First, to ensure data quality, the absence of random distribution in the dataset is checked using an autocorrelation diagram. The absence of a stationary phenomenon is assessed through a partial autocorrelation function calculation [11]. Next, the data were examined for periodicity via spectral analyses, specifically the Lomb and Scargle periodogram [38]. This periodogram establishes a significance threshold ($p = 0.95$). Finally, rhythmicity is confirmed by the Cosinor model, utilizing the period identified by the Lomb and Scargle periodogram [39]. For a given period, the model is expressed as: $Y(t) = A\cos(\pi t/\tau + \varphi) + M + \varepsilon(t)$, where A represents the amplitude, φ is the acrophase, τ denotes the period, M is the mesor and ε is the relative error. Two critical tests validate the calculated model and the existence of a rhythm: the elliptic test must be rejected, and the probability for the null amplitude hypothesis must be <0.05. A chronobiometric parameter was computed: the percent rhythm (PR, %), the percentage of cyclic behaviour explained by the model. For each series, the VOA dataset is examined for rhythmicity within the circadian range ($\tau = 24 \pm 4$ h) and in the ultradian range ($\tau < 20$ h). These analyses were conducted at the group level (EU1 + EU2, $n = 24$ individuals).

Rhythmic analysis of clock genes expression was performed using the R package 'RAIN' [40,41]. RAIN was specifically designed to detect rhythms in biological datasets independent of waveform utilizing a non-parametric approach [41]. Periods are tested in the ultradian (12 h ± 2 h) and daily/circadian (24 h ± 4 h) period ranges and are considered significant if $p < 0.05$. Significant rhythms in the daily/circadian period ranges are labelled as 'daily' under L:D entrainment and 'circadian' under D:D.

3. Results

3.1. Identification of genes involved in the circadian machinery of *O. edulis*

3.1.1. Identification of genes and their protein domains in *O. edulis*

The investigation of the *O. edulis* reference genome assembly [30], combined with research on protein domains and phylogeny, led to the identification of thirteen orthologues putatively involved in or related to the circadian clock machinery. These include ten circadian clock genes (*OeClock*, *OeBmal1*, *OePer1*, *OeTim1*, *OeCry2*, *OeRev-erb*, *OeRor*, *OeDbt*, *OeCwo*, *OeShag*), one gene involved in melatonin synthesis (*OeHiomt*), and two photoreceptor genes (*OeCry1* and *OeOpn4*) (refer to the complete list with accession numbers in electronic supplementary material, table S1). The identification and putative function of all 13 genes of interest were validated based on their protein domain similarities, with the domains of *O. edulis* genes shown in figure 3 and the corresponding domains from other species presented in electronic supplementary material, figure S2.

First, we identified OeCLOCK and OeBMAL1 as the putative positive components of the first transcriptional and translational feedback loop in *O. edulis*. A 677 aa *OeClock* sequence (XP_048756709.1) was identified. A 546 aa *OeBmal1* sequence (XP_048730810.1) was also identified. Both sequences contain a basic helix-loop-helix (bHLH) domain (figure 3), responsible for interactions with the E-box, and PAS and PAC domains, mediating CLOCK-BMAL1 dimerization (figure 3). These domains are highly conserved across other animal species and within Bivalvia (electronic supplementary material, figure S2), supporting the formation of the OeCLOCK/OeBMAL1 dimer in *O. edulis*.

We identified OePER1, OeTIM1 and OeCRY2 as the putative negative elements of the first transcriptional and translational feedback loop in *O. edulis*. The 1314 aa *OePer1* sequence (XP_048730714.1) contained highly conserved protein domain regions with the heterodimerization domains PAS and PAC, and Period protein 2/3 C-terminal region involved in the binding between PER and CRYs in vertebrates [42,43]. By contrast to *OeClock* and *OeBmal1*, no bHLH domain was identified in *OePer1* (figure 3), reinforcing its classification as a PERIOD protein that, unlike CLOCK and BMAL, functions in the main transcriptional and translational feedback loop without directly binding to DNA. The 949 aa *OeTim1* sequence (XP_048747482.1) and the 1255 aa *OeCry2* sequence (XP_048913721.1) contained typical domains (figure 3), including a FAD-Binding domain, a DNA photolyase domain and a Suppressor of forked protein (Suf) domain for *OeCry2*.

We also identified *OeRor* and *OeRev-erb* as orthologues of *ror* (*HR3* in insects) and *rev-erb*, which are known to enhance the robustness of the circadian clock by regulating *Bmal* transcription [3,44]. The 502 aa *OeRor* sequence was identified (XP_056002619.1), containing Retinoid-related orphan receptors (figure 3). The 1089 aa sequence of *OeRev-erb* (XP_048918733.1) was identified, containing a nuclear receptor DNA-binding domain (NR_DBD_REV_ERB) and a nuclear receptor ligand-binding domain (figure 3). Additional clock-related components have been identified: a 426 aa *OeDbt* sequence (XP_048904376.1) contains a Casein kinase 1 Ser/Thr kinase domain, identified as a *doubletime* orthologue known to play a role in the phosphorylation of PERIOD and TIMELESS in *Drosophila* [1,45]. An *OeCwo* sequence (XP_048885347.1), 376 aa in length and containing an Orange domain, is identified as a *cwo* orthologue described as an inhibitor of the CLOCK/BMAL heterodimer, thereby monitoring the amplitude of clock activity [46]. An *OeShag* sequence (XP_048923210.1), 412 aa in length and containing a Glycogen synthase kinase 3 catalytic domain, was identified (figure 3).

A 410 aa *OeHiomt* sequence (XP_048878998.1), containing a plant O-methyltransferase dimerization domain and an O-methyltransferase domain, was identified as a *hiomt* orthologue implicated in the synthesis of melatonin (*N*-acetyl-5-methoxytryptamine) from serotonin [47].

Finally, photoreceptor genes were identified: the 545 aa *OeCry1* sequence (XP_048728452.1) was isolated and contained conserved DNA photolyase and FAD-binding domains involved in the photoreduction of the flavin adenine dinucleotide (FAD) component, characteristic of photolyase/CRY family proteins [46,47] (figure 3). The *OeOpn4* sequence (XP_048908333.1), 384 aa in length, was identified as an *opsin4* (*melanopsin*) orthologue, a photopigment involved in detecting irradiance levels [48–50]. It contains a GPCR, rhodopsin-like, 7-transmembrane (7TM) domain characteristic of both *Opn3* and *Opn4* proteins. BLAST analysis further supported its annotation as an *Opn4*-like gene, showing higher similarity to annotated *Opn4* (*melanopsin*) sequences, including *Mya arenaria* (XP_052777205.1; query cover: 93%, identity: 42%, E-value: 4e-96) and *Homo sapiens* (AAI13559.1; query cover: 84%, identity: 34%, E-value: 7e-46).

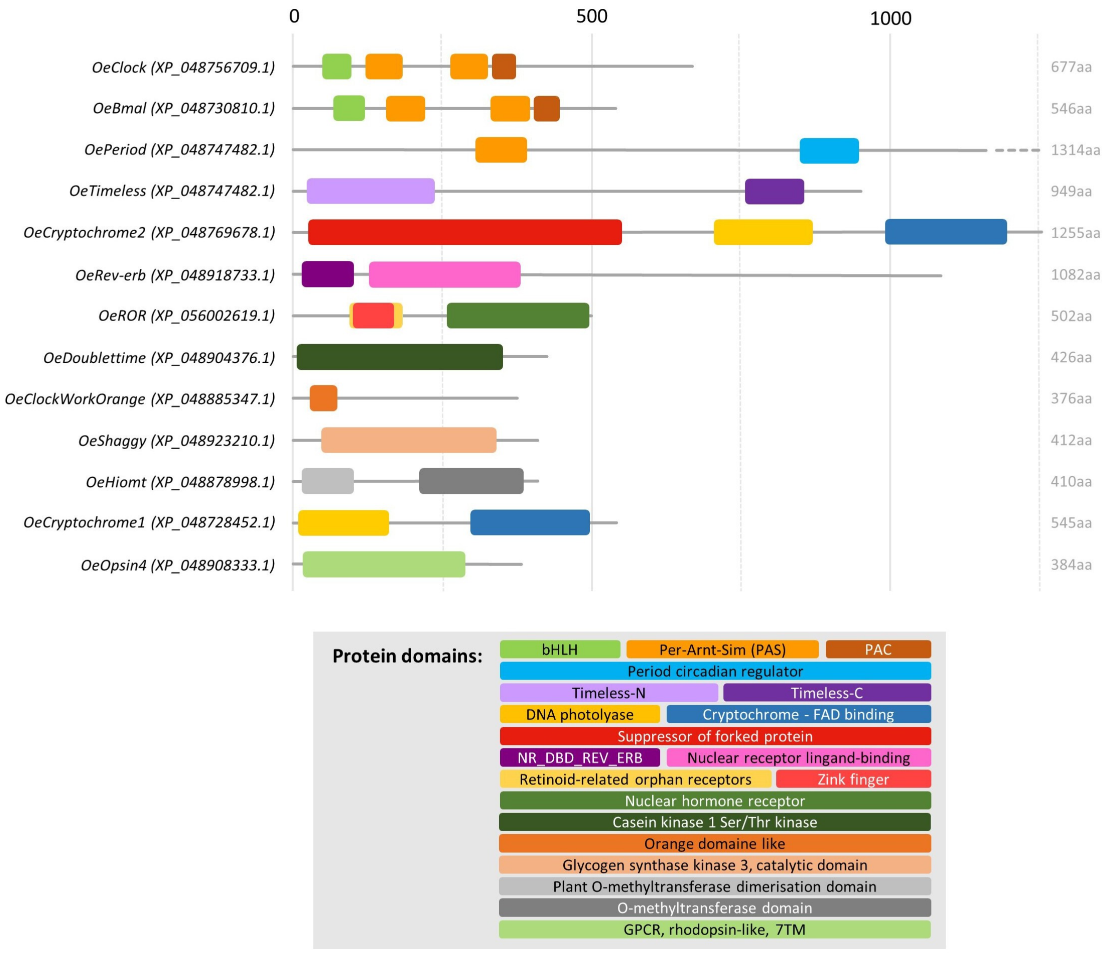

Figure 3. Investigation of protein domains in *O. edulis***.** Protein domains for *OeClock*, *OeBmal1*, *OePeriod*, *OeTimeless*, *OeCryptochrome2*, *OeRev-erb*, *OeRor*, *OeDoubletime*, *OeClockWorkOrange*, *OeShaggy*, *OeHiomt*, *OeCryptochrome1* and *OeOpsin4*. Grey lines represent the protein length. Coloured bars represent protein domains. Protein domain abbreviations: basic helix-loop-helix (bHLH) domains, Proline-Rich, Arabinogalactan Proteins, and Conserved Cysteines (PAC) domains, Timeless N-terminal (Timeless-N) domains, Timeless C-terminal (Timeless-C) domains, nuclear receptor DNA-binding (NR_DBD_REV_ERB) domain.

3.1.2. Phylogenetic analyses and similarity to other taxa

Phylogenetic analysis revealed relationships of genes identified in *O. edulis* to orthologues within the animal kingdom and the Bivalvia class. First, for the putative positive components of the first transcriptional and translational feedback loop identified in *O. edulis*, *OeClock* shares closer similarity to mammalian CLOCK than insect sequences (figure 4); for instance, it shares 55% similarity with the mouse *Mus musculus Clock*-like (NP_001292151.1) and 48% with the fruit fly *D. melanogaster Clock*-like (AAD10630.1). At the Bivalvia level, it shares 82% similarity with the Pacific oyster *C. gigas Clock*-like (10KX15642.1). *OeBmal1* clustered closer to vertebrate-type BMAL1 clades and at the Bivalvia level, it shares 87% similarity with *C. gigas Bmal1*-like (XP_034328823.1) (figure 4).

Then for the putative negative elements of the first transcriptional and translational feedback loop identified in *O. edulis*, *OePer1* was closer to insect PER orthologues (figure 4). At the Bivalvia level, it shared 65% and 63% similarity with *Period* orthologues from *C. virginica* (XP_022345652.1) and *C. gigas* (XP_011434453.2), respectively (figure 4). *OeTim1* was phylogenetically closer to the insect TIM1 orthologues (figure 4) and shared 69% similarity with a *C. gigas Timeless* orthologue (XP_011434769.2) (figure 4).

Phylogenetic analysis was also instrumental in distinguishing *OeCry1* and *OeCry2* and inferring their respective functions. *OeCry2* was found to be closer to mammalian-type CRY than to *Drosophila*-type CRY (figure 4), suggesting that *OeCry2* acts as a transcriptional repressor in the core clock feedback loop of *O. edulis* [51] (figure 4). *OeCry1* grouped closer to the *Drosophila*-type CRY1 (figure 4), suggesting a circadian photoreception role in *O. edulis*. Specifically, we found 86% similarity between

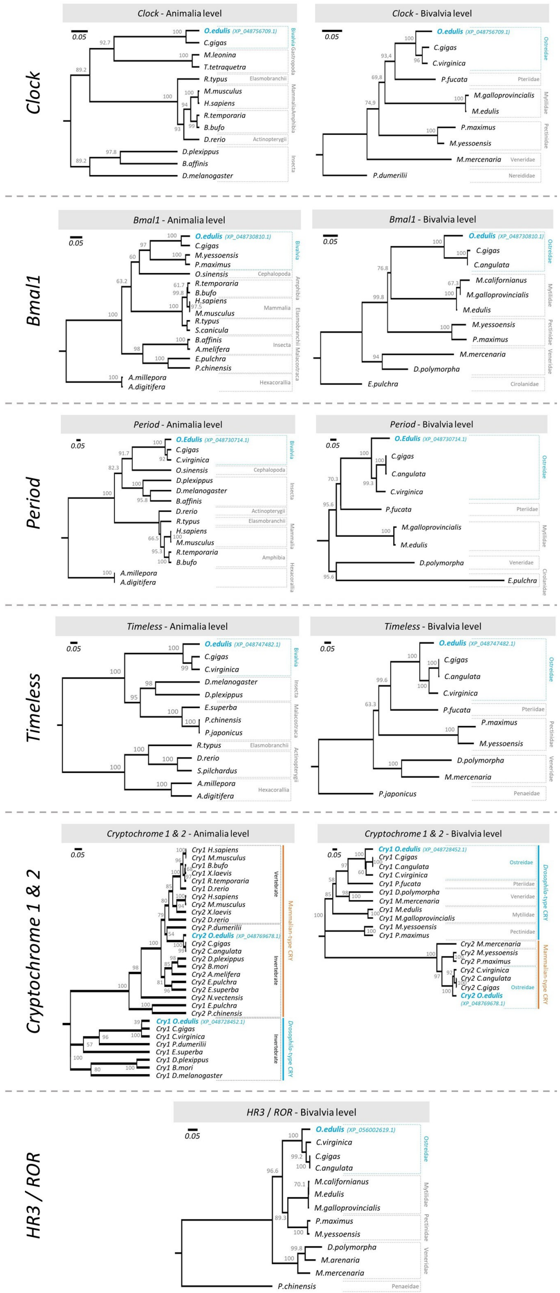

Figure 4. Phylogenetic position of *OeClock, OeBmal1*, *OePeriod*, *OeTimeless*, *OeCryptochrome1*, *OeCryptochrome2* and *OeRor* within the animal kingdom and the Bivalvia class. Rooted phylogenetic trees of *Clock*, *Bmal1*, *Period*, *Timeless*, *Cryptochrome1*, *Cryptochrome2* and *ROR* sequences within the animal kingdom and the Bivalvia class. The *O.edulis* sequences and the associated family or class are depicted in clear blue. The numbers on the branches indicate bootstrap values provided by the maximum likelihood method with 1000 bootstrap replicates. Abbreviations for each species used in this figure: *Acropora digitifera* (*A. digitifera*), *Acropora millepora* (*A. millepora*), *Apis mellifera* (*A. mellifera*), *Bombus affinis* (*B. affinis*), *Bombyx mori* (*B. mori*), *Bufo bufo* (*B. bufo*), *Crassostrea angulata* (*C. angulata*), *Crassostrea gigas* (*C. gigas*), *Crassostrea virginica* (*C. virginica*), *Danaus plexippus* (*D. plexippus*), *Danio rerio* (*D. rerio*), *Dreissena polymorpha* (*D. polymorpha*), *Drosophila melanogaster* (*D. melanogaster*), *Euphausia superba* (*E. superba*), *Eurydice pulchra* (*E. pulchra*), *Homo sapiens* (*H. sapiens*), *Mercenaria mercenaria* (*M. mercenaria*), *Mizuhopecten yessoensis* (*M. yessoensis*), *Mus musculus* (*M. musculus*), *Mytilus californianus* (*M. californianus*), *Mytilus edulis* (*M. edulis*), *Mytilus galloprovincialis* (*M. galloprovincialis*), *Mya arenaria* (*M. arenaria*), *Nematostella vectensis* (*N. vectensis*), *Octopus sinensis* (*O. sinensis*), *Ostrea edulis* (*O. edulis*), *Pecten maximus* (*P. maximus*), *Penaeus chinensis* (*P. chinensis*), *Penaeus japonicus* (*P. japonicus*), *Pinctada fucata* (*P. fucata*), *Platynereis dumerilii* (*P. dumerilii*), *Rana temporaria* (*R. temporaria*), *Rhincodon typus* (*R. typus*), *Sardina pilchardus* (*S. pilchardus*), *Tritonia tetraquetra* (*T. tetraquetra*), *Xenopus laevis* (*X. laevis*).

OeCry1 and *C. gigas Cry1*-like (ANJ02841.1) and 56% similarity with the marine annelid *Platynereis dumerilii Cry1*-like (UUF95169.1).

Finally, the phylogenetic tree of *OeRor* at the Bivalvia level revealed important similarity between *O. edulis* and *Ostreidae*, *Mytilidae* and *Pectinidae*. Specifically, it shared 85% and 65% similarity with the probable *ror* orthologues of *C. gigas* (XP_034321280.1) and *P. maximus* (XP_033724975.1), respectively (figure 4). The phylogenetic analysis of ROR was restricted to bivalves due to the limited number of confidently identified ROR sequences available at the broader Animalia level.

3.2. *O. edulis* valve activity

Figure 2 illustrates the actograms of the mean VOA during two 17-day experiments and the corresponding results of chronobiological analyses based on the oysters from the two EUs (n = 24 individuals per experiment). After a 7-day pre-exposure (12 L:12 D), two light regimes were tested, each for 10 days: 12 L:12 D (L:D experiment) and D:D (D:D experiment) (hourly individual VOA data are accessible in the electronic supplementary material, dataset S2). During the pre-exposure to the 12 L:12 D regime, oysters exhibited a significant daily rhythm of 24.1 ± 0.02 h and 24.4 ± 0.02 h in the L:D experiment and D:D experiment, respectively, with a rhythm robustness percentage (PR) averaging 73.2%. In the following L:D exposure of the L:D experiment, VOA showed a significant daily rhythm of about 23.9 ± 0.02 h, with a PR of 73.5%. This rhythmicity is comparable with that observed during the pre-exposure with the same 12 L:12 D regime. In the D:D experiment, used to test the endogenous circadian behavioural rhythm, *O. edulis* demonstrated under D:D exposure a persistent rhythm within the circadian range (20–28 h) of approximately 26.8 ± 0.02 h, with an associated PR of 38.5%.

3.3. Gene expression in gills and labial palps

Table 1 presents the results of RAIN analysis used to assess rhythmicity in the expression of the putative core circadian clock genes (*OeClock*, *OeBmal*, *OePer1*, *OeTim1*, *OeCry2*), genes involved in secondary loops of the circadian clock (*OeRev-erb*, *OeRor*, *OeCwo*), as well as genes involved in post-translational regulations of the circadian clockwork (*OeDbt*, *OeShag*), a gene involved in melatonin synthesis (*OeHiomt*), and photoreceptor genes (*OeCry1* and *OeOpn4*) in the gills and labial palps of *O. edulis* under L:D and D:D conditions (representative temporal expression profiles are provided in electronic supplementary material, figure S3, and dataset S3 provides detailed gene expression data in gills and labial palps during L:D and D:D experiments). Results presented in electronic supplementary material, figure S3, showed that all the studied genes are expressed in both tissues. Rhythm analysis conducted using RAIN algorithm revealed daily/circadian (24 ± 4 h) and ultradian (12 ± 2 h) period ranges of oscillations in gene expression for both gills and labial palps (table 1). Firstly, in the gills under L:D conditions, five genes exhibited significant daily rhythmicity, including *OeBmal1*, *OeRor*, *OeCwo*, *OeShag* and *OeOpn4*; while *OeClock*, *OeTim1*, *OeCry2* and *OeCry1* displayed significant ultradian rhythmicity; and *OePer1*, *OeRev-erb*, *OeDbt* and *OeHiomt* showed no significant rhythmicity (table 1). The expression profiles of *OeBmal1*, *OeTim1*, *OeCry2*, *OeRor*, *OeDbt*, *OeCwo* and *OeCry1* showed a nocturnal peak (ZT17, ZT19 or ZT21) while *OeOpn4* displayed two peaks, one at the beginning of the day (ZT1) and another in the middle of the day (ZT7) (electronic supplementary material, figure S3). Under D:D conditions, only *OeOpn4* maintained a rhythm in the circadian range, and ultradian rhythmicity was observed for *OeClock*, *OeCry2*, *OeRev-erb*, *OeRor*, *OeDbt*, *OeShag* and *OeCry1* (table 1). *OeOpn4* only maintained the peak of expression at the beginning of the subjective day (CT1) (electronic supplementary material, figure S3). For *OeBmal1*, *OePer1*, *OeRev-erb*, *OeRor*, *OeDbt*, *OeCwo*, *OeShag* and *OeCry1*, the nocturnal peak shifted to the subjective early night (CT13) (electronic supplementary material, figure S3). Secondly, in the labial palps, rhythmic expression was more pronounced than in the gills under both L:D and D:D regimes. Under L:D condition, significant daily rhythms were detected for seven genes: *OeBmal1*, *OePer1*, *OeTim1*, *OeCry2*, *OeRev-erb*, *OeDbt* and *OeOpn4*, with three of them (*OeBmal1*, *OeDbt*, *OeOpn4)* also showing ultradian rhythm, while *OeRor*, *OeCwo*, *OeShag* and *OeCry1* showed only ultradian expression, and *OeClock* and *OeHiomt* showed no significant rhythm (table 1). Notably, *OeOpn4* exhibited profiles comparable to those in the gills (electronic supplementary material, figure S3). Under D:D conditions, seven genes exhibited a circadian rhythm in labial palps: *OeCry2*, *OeRor*, *OeCwo*, *OeShag*, *OeHiomt*, *OeCry1* and *OeOpn4*, while nine genes showed ultradian rhythms: *OeBmal1*, *OeTim1*, *OeCry2*, *OeRev-erb*, *OeRor*, *OeDbt*, *OeCwo*, *OeShag* and *OeHiomt*, including five genes (*OeCry2*, *OeRor*, *OeCwo*, *OeShag*, *OeHiomt)* with both circadian and ultradian rhythms (table 1). A peak in gene expression was observed during the subjective early night (CT13) for *OeBmal1*, *OePer1*, *OeCry2*, *OeDbt*, *OeCwo*, *OeShag*, *OeHiomt* and *OeCry1*, while *OeOpn4* showed peaks during the subjective day (CT1) (electronic supplementary material, figure S3).

4. Discussion

In this study, data mining and protein domain analysis identified 13 key components putatively involved in the circadian clock functioning of the flat oyster *Ostrea edulis.* These include orthologues of circadian clock genes, light reception genes and a gene related to melatonin synthesis. Phylogenetic analyses revealed that the identified gene sequences shared strong homology with genes described in circadian clock models from other species, indicating conservation across diverse taxa. Notably, our findings suggest the presence of two distinct types of cryptochromes in *O. edulis*: *OeCry2*, which would be directly implicated in the main circadian loop, and *OeCry1*, which would function as a circadian photoreceptor. At the molecular level, rhythmic mRNA expression patterns were observed in gill and labial palp tissues, with some genes exhibiting daily and/or ultradian rhythms under L:D and D:D conditions, suggesting a plastic and self-sustained mechanism. Although endogenous clocks have been described in some marine invertebrates [52,53], including a few bivalves [16], their functional characterization in oysters remains limited. Our findings in *O. edulis* expand the phylogenetic range of bivalves and demonstrate endogenous circadian regulation of valve behaviour with synchronized daily valve activity under L:D conditions, as well as a maintained circadian rhythm in free-running conditions (D:D). These behavioural rhythms, observed as an output of the molecular clock, provide strong evidence for a functional endogenous clock mechanism in this species.

4.1. Circadian clock genes in *O. edulis*

This study identified five genes in *O. edulis* as orthologues of genes involved in the core loop of the circadian clock in other species: *OeClock*, *OeBmal1*, *OePer1*, *OeTim1* and *OeCry2*. These genes are conserved across major metazoan lineages, including vertebrates (Deuterostomia), ecdysozoans such as *D. melanogaster* [54] and *Euphausia superba* [52], and lophotrochozoans such as *P. dumerilii* [53] and *C. gigas* [16]. They form positive and negative feedback loops, producing a self-sustained oscillation for approximately 24 h period, regulated by environmental cues [8,9]. The presence of these genes suggests a similar function of *O. edulis*'s circadian core clock. Additionally, *OeRor* and *OeRev-erb* were recognized as orthologues of *ror* and *rev-erb* known to regulate *Bmal1* transcription and enhance clock robustness [3,44]. In vertebrates and phylogenetically close species such as *C. gigas*, *rev-erb* has been described as an inhibitor, while *ror* acts as an activator of *Bmal1* expression [55,56]. We also identified additional genes, orthologues of clock genes known in *Drosophila* to be involved in the secondary loop of the circadian clock (*Cwo*), or genes involved in post-translational regulations of the circadian clockwork (*Dbt* and *Shag*) [45,46]. Though less studied in marine organisms, these genes have been identified in oyster species such as *Crassostrea angulata* for *shaggy* [57] as well as in the copepod *Calanus finmarchicus* or the scallop *Pecten yessoensis* for *doubletime* [58,59]. Their identification in *O. edulis* could indicate their crucial role and implication in the molecular clock regulation mechanism.

We identified two types of cryptochromes in *O. edulis*, *OeCry1* and *OeCry2*, both possessing conserved protein domains characteristic of photolyase/CRY family proteins [60,61]. Cryptochromes are classified by their function. The first type, *OeCry1*, is referred to as '*Drosophila*-type' cryptochromes, and serves as blue-light-sensitive photoreceptors. They provide environmental input to the core clock by interacting with the TIM1-PER heterodimer in a light-dependent manner promoting light-induced degradation of TIM1 [62–66]. By contrast, the second type, *OeCry2*, is referred to as 'mammalian-type' cryptochromes and acts as non-photosensitive repressors that inhibit CLOCK/BMAL1 activity [7,67]. Phylogenetic analysis grouped *OeCry1* with the '*Drosophila*-type' cryptochromes and *OeCry2* with the 'mammalian-type' cryptochromes. The identification of the phylogenetic trees of these two cryptochrome types, supports 'butterfly-type' molecular mechanisms in *O. edulis* described in the monarch butterfly *Danaus plexippus* [67], as suggested in the marine copepod *C. finmarchicus* [68,69] or the oyster *C. gigas* [16], where the principal positive feedback loop involves the CLOCK/BMAL1 heterodimer, and the primary negative feedback loop involves the TIM1/PER/CRY2 complex, with CR1 interacting with TIM1 for photo-entrainment.

Table 1. Detailed results of chronobiological analysis in expression levels of clock genes in *Ostrea edulis* gills and labial palps. Results of the RAIN analysis are shown for both light:dark (L:D) and constant darkness (D:D) experiments. For each gene and condition, the detected rhythm period (Per.) is indicated when significant rhythmicity was found in the daily/circadian (20–28 h) or ultradian (10–14 h) ranges. Significant p-values ($p < 0.05$) are indicated in bold, and the peak time of maximal expression is reported in ZT/CT. ZT: zeitgeber time; CT: circadian time.

	genes	gills circadian range (20–28 h) Per.	gills circadian p-value	gills circadian peak	gills ultradian range (10–14 h) Per.	gills ultradian p-value	gills ultradian peak	labial palps circadian range (20–28 h) Per.	labial palps circadian p-value	labial palps circadian peak	labial palps ultradian range (10–14 h) Per.	labial palps ultradian p-value	labial palps ultradian peak
L:D	*OeClock*	ns	0.191	ns	14	**0.009**	ZT19	ns	0.072	ns	ns	0.070	ns
	OeBmal1	20	**0.044**	ZT17	ns	0.276	ns	20	**0.046**	ZT17	14	**0.040**	ZT17
	OePer1	ns	0.090	ns	ns	0.056	ns	22	**0.038**	ZT21	ns	0.127	ns
	OeTim1	ns	0.107	ns	ns	0.055	ns	22	**0.038**	ZT5	ns	0.127	ns
	OeCry2	ns	0.221	ns	ns	0.075	ns	22	**0.036**	ZT5	ns	0.127	ns
	OeRev-erb	ns	0.849	ns	ns	0.099	ns	22	**0.017**	ZT11	ns	0.158	ns
	OeRor	20	**0.003**	ZT17	14	**0.012**	ZT17	ns	0.053	ns	14	**0.017**	ZT11
	OeDbt	ns	0.778	ns	10	**0.035**	ZT19	22	**0.046**	ZT5	14	**0.040**	ZT5
	OeCwo	26	**0.010**	ZT17	ns	0.751	ns	ns	0.079	ns	14	**0.040**	ZT17
	OeShag	22	**0.002**	ZT19	ns	0.761	ns	ns	0.064	ns	14	**0.022**	ZT5
	OeHiomt	ns	0.289	ns	ns	0.149	ns	ns	0.146	ns	ns	0.076	ns
	OeCry1	ns	0.174	ns	14	**0.033**	ZT21	ns	0.088	ns	14	**0.017**	ZT5
	OeOpn4	20	**0.000**	ZT1	ns	0.451	ns	22	**0.046**	ZT7	14	**0.040**	ZT7
D:D	*OeClock*	ns	0.425	ns	12	**0.024**	CT5	ns	0.084	ns	ns	0.059	ns
	OeBmal1	ns	0.343	ns	ns	0.124	ns	ns	0.088	ns	14	**0.017**	CT13
	OePer1	ns	0.259	ns	ns	0.072	ns	ns	0.093	ns	ns	0.127	ns
	OeTim1	ns	0.171	ns	12	**0.028**	CT5	ns	0.064	ns	14	**0.022**	CT23
	OeCry2	ns	0.425	ns	ns	0.255	ns	22	**0.038**	CT13	14	**0.010**	CT13

(*Continued.*)

Table 1. (*Continued.*)

genes	circadian range (20–28 h)			ultradian range (10–14 h)			circadian range (20–28 h)			ultradian range (10–14 h)		
	Per.	*p*-value	peak	Per.	*p*-value	peak	Per.	*p*-value	peak	Per.	*p*-value	peak
	gills						labial palps					
OeRev-erb	ns	0.068	ns	14	**0.037**	CT13	ns	0.064	ns	14	**0.022**	CT23
OeRor	ns	0.845	ns	ns	0.060	ns	22	**0.046**	CT23	14	**0.040**	CT23
OeDbt	ns	0.425	ns	ns	0.348	ns	ns	0.064	ns	14	**0.022**	CT13
OeCwo	ns	0.198	ns	ns	0.341	ns	20	**0.046**	CT13	14	**0.040**	CT13
OeShag	ns	0.109	ns	10	**0.000**	CT13	20	**0.017**	CT3	14	**0.031**	CT3
OeHiomt	ns	0.069	ns	ns	0.401	ns	22	**0.049**	CT13	14	**0.035**	CT13
OeCry1	ns	0.828	ns	12	**0.031**	CT13	22	**0.036**	CT3	ns	0.070	ns
OeOpn4	28	**0.014**	CT1	ns	0.232	ns	20	**0.027**	CT1	ns	0.076	ns

The study also allowed for identification of another putative light reception gene, *OeOpn4*, an orthologue of *opsin4* (*melanopsin*), which is involved in the detection of light intensity [48–50], highlighting the potential of opsins for exploring the photoreceptive repertoire contributing to circadian regulation in *O. edulis*. The identification of this gene, along with *OeCry1*, which is known to be involved in the detection of short wavelengths of light, in the blue range, suggests that blue light could play a role in the synchronization of the endogenous clock through non-visual photoreceptors in *O. edulis*. Although direct evidence for wavelength sensitivity in *O. edulis* is lacking, previous studies in bivalves [70,71] indicate light-mediated behavioural rhythms and putative photoreceptors, supporting a potential role of light perception in circadian regulation.

Finally, we identified *OeHiomt*, which is predicted to encode hydroxyindole-O-methyltransferase (HIOMT), an enzyme involved in melatonin (*N*-acetyl-5-methoxytryptamine) synthesis [47]. Melatonin is an evolutionarily conserved hormone implicated in regulating temporal rhythms across daily, lunar and annual cycles in various invertebrates, vertebrates, plants and bacteria [72–74]. The presence of *OeHiomt* highlights the potential role of melatonin in the circadian machinery in *O. edulis*.

Overall, the identification of the circadian clock molecular components and validation of conserved protein domains indicate that the endogenous clock in *O. edulis* may share a similar architecture with phylogenetically close species such as *C. gigas*. To go further, we investigated the functionality of the circadian clock in *O. edulis*.

4.2. Investigation of the functionality of the circadian clock

We then investigated whether the identified circadian clock genes are expressed in two different tissues (gills and labial palps) of *O. edulis*, and if they are rhythmically expressed. We also investigated the temporal expression level of all the other genes identified in this study, putatively under clock control, and we concomitantly studied the temporal valve behaviour patterns of *O. edulis*, also putatively under clock control. Oyster valve opening is required to filter water, allowing oxygen supply and nutritional physiological processes in which gills and labial palps are actively involved. Gills have a role in respiration but also in nutrition as they permit the transport of food particles to the labial palps, while labial palps manage the final selection and transfer of food particles to the digestive tract [75].

The observed rhythmic gene expression and behaviour support the existence of a functional endogenous oscillator. Interestingly, while valve activity showed clear daily (under L:D) and circadian (under D:D) rhythms as described in a previous study [27], the temporal expression patterns of both circadian clock gene and putative clock-controlled genes were more variable, showing some daily/circadian rhythms but also ultradian ones, as well as bimodal (both daily/circadian and ultradian periodicities) and arhythmic patterns, depending on genes and tissues. This discrepancy between behavioural and molecular rhythms, and between the two tissues, may be attributed to tissue-specific oscillations [76]. It may be suggested that the adductor muscle, directly involved in the valve activity, expresses a different profile of clock gene oscillations from those observed in gills and labial palps. Furthermore, the tissue-specific physiological functions of gills and labial palps may require distinct temporal organization, explaining differences in expression profiles observed in both core circadian clock genes and putative clock-controlled genes. Additionally, it has to be noted that the molecular approach is more sensitive to individual variability than the behavioural approach due to methodological reasons. Time series sampling for molecular investigation requires sacrificing individuals at each time point. Furthermore, both the number of oysters per time point (eight individuals) and the sampling frequency are limited by logistical reasons. By contrast, the behavioural analysis, based on the continuous recording of the same 24 individuals throughout the whole experiment, is more efficient in revealing a rhythmic pattern. Nevertheless, despite individual variability, the different rhythmicities (daily/circadian, ultradian or bimodal) observed at the molecular level may reflect an intrinsic plasticity and or lability of the circadian clock's functioning in *O. edulis*.

4.3. A plastic and labile clock in *O. edulis*

The clock plasticity observed in this study at the molecular level is in accordance with a previous study where the circadian behaviour of *O. edulis* was described as labile and plastic [27]. This plasticity may reflect an adaptive feature aligned with Enright's hypothesis of a single, flexible oscillator governing multiple temporal rhythms in marine organisms, allowing adaptation to both daily and tidal environmental cycles [77]. This hypothesis is supported by studies of species like the oyster

C. gigas [17,78,79] or the copepod *C. finmarchicus* [58]. In our study, and in the absence of tidal entrainment, the ultradian rhythms could be interpreted as circatidal rhythms, revealing the putative endogenous capacity of clock components to be entrained by tidal environmental cues. The oysters used in this study used to be cultivated in natural subtidal conditions; however, it does not exclude that they may have been exposed to tidal forces other than emersion. As observed in *C. gigas*, bimodal rhythms of circadian clock genes expression are also expressed, i.e. a mix between both daily/circadian and tidal periodicities [17]. However, unlike what is observed under pure L:D entrainement in *C. gigas* [17], a relatively high number of circadian genes are found to show ultradian rhythms under the same conditions in *O. edulis*. Further studies combining both daily and tidal *zeitgebers* would be necessary to better understand and characterize the molecular clock functioning and entrainment in *O. edulis*. In the field, the clock plasticity may confer advantages, allowing marine organisms to adapt to their complex biotope, which is subjected to multiple cycles [14]. It could also be advantageous for adaptation to temperature shifts due to global warming, as discussed in [27]. However, it could also increase sensitivity to anthropogenic pressures such as artificial light at night, potentially influencing coastal populations of *O. edulis*. Understanding this vulnerability is crucial for conservation efforts to enhance the species' resilience to environmental changes.

5. Conclusion

This study identified the orthologues of key circadian clock components in *Ostrea edulis*, highlighting the conserved structural and functional domains of their protein sequences. Expression profiling of these clock genes has provided new insights into the molecular mechanisms underlying clock-driven phenotypes in this bivalve. Understanding the molecular basis of these biological rhythms is essential for enhancing our comprehension of this European native oyster, as well as for better understanding its response to environmental cycles and improving conservation strategies for the species. The labile aspect of the clock discussed in this study may facilitate further adaptation to temperature shifts due to global warming. On the contrary, the labile element of the clock may also reinforce negative aspects of anthropogenic activity, such as the expansion of artificial light at night. In this perspective, our findings present a first approach. They will facilitate further investigation of circadian clock genes in *O. edulis*, providing genetic resources for exploring the genetic mechanisms of this biological clock. However, to fully characterize the molecular clock mechanism in *O. edulis*, further functional approaches, in both laboratory and natural conditions, will be necessary to better define the relationships between these genes and their specific roles within the clock mechanism in *O. edulis*.

Ethics. All research conducted in this study adhered to French legislation and followed international ethical standards.

Data accessibility. The sequences of genes used to construct phylogenetic trees can be found via accession numbers given in electronic supplementary material, table S1 for *Ostrea edulis* and dataset S1 for other species. Hourly individual VOA data from L:D and D:D laboratory experiments are accessible in electronic supplementary material, dataset S2. Gene expression data in gills and labial palps during L:D and D:D laboratory experiments are accessible in electronic supplementary material, dataset S3. Electronic supplementary material, table S2, provides detailed results of RAIN analysis in expression levels of clock genes in *Ostrea edulis* gills and labial palps.

Supplementary material is available online [80].

Declaration of AI use. We have not used AI-assisted technologies in creating this article.

Authors' contributions. A.L.M.: conceptualization, data curation, formal analysis, investigation, methodology, validation, visualization, writing—original draft, writing—review and editing; L.P.: conceptualization, funding acquisition, methodology, project administration, supervision, validation, writing—review and editing; D.T.: conceptualization, funding acquisition, methodology, project administration, supervision, validation, writing—review and editing; F.D.: formal analysis, writing—review and editing; A.B.: formal analysis, writing—review and editing; B.P.: conceptualization, funding acquisition, methodology, project administration, supervision, validation, writing—review and editing; B.M.: conceptualization, funding acquisition, methodology, project administration, supervision, validation, writing—review and editing.

All authors gave final approval for publication and agreed to be held accountable for the work performed therein.

Conflict of interest declaration. We declare we have no competing interests.

Funding. A.L.M. was supported by a grant awarded to B.M. and B.P. via AWI Inspires—International Science Program for Integrative Research in Earth Systems. The study contributes to the Helmholtz Research Program 'Changing Earth—sustaining our future' of the research field Earth and Environment of the Helmholtz Association, Topic 6, Subtopic 6.1 and 6.2 as well as Topic 4, Suptopic 4.2. The project was supported by the 'PHC PROCOPE' programme via the project 'OysterClock' (project-ID: 57701739), funded by the French Ministry for Europe and

Foreign Affairs, the French Ministry for Higher Education and Research and the German Academic Exchange Service (DAAD). The work was also supported by the French National Research Agency (ANR), LUCIOLE project (ANR-22-CE34-0010-01).

Acknowledgements. We thank Yannick Geerebaert for his help during the setup of the experiment. We thank Christophe Klopp for his help on the bio-informatic and data mining work. We thank Laure Bellec for her help on the phylogenetic work. We thank Cerise Daffe for the help during the design of the primers. We thank Kristin Tessmar-Raible and Stephane Pouvreau for valuable discussions.

References

1. Andreatta G, Tessmar-Raible K. 2020 The still dark side of the moon: molecular mechanisms of lunar-controlled rhythms and clocks. *J. Mol. Biol.* **432**, 3525–3546. (doi:10.1016/j.jmb.2020.03.009)
2. Bell-Pedersen D, Cassone VM, Earnest DJ, Golden SS, Hardin PE, Thomas TL, Zoran MJ. 2005 Circadian rhythms from multiple oscillators: lessons from diverse organisms. *Nat. Rev. Genet.* **6**, 544–556. (doi:10.1038/nrg1633)
3. Zhang EE, Kay SA. 2010 Clocks not winding down: unravelling circadian networks. *Nat. Rev. Mol. Cell Biol.* **11**, 764–776. (doi:10.1038/nrm2995)
4. Dubruille R, Emery P. 2008 A plastic clock: how circadian rhythms respond to environmental cues in *Drosophila*. *Mol. Neurobiol.* **38**, 129–145. (doi:10.1007/s12035-008-8035-y)
5. Hardin PE. 2005 The circadian timekeeping system of *Drosophila*. *Curr. Biol.* **15**, R714–22. (doi:10.1016/j.cub.2005.08.019)
6. Zhang L, Hastings MH, Green EW, Tauber E, Sladek M, Webster SG, Kyriacou CP, Wilcockson DC. 2013 Dissociation of circadian and circatidal timekeeping in the marine crustacean *Eurydice pulchra*. *Curr. Biol.* **23**, 1863–1873. (doi:10.1016/j.cub.2013.08.038)
7. Yuan Q, Metterville D, Briscoe AD, Reppert SM. 2007 Insect cryptochromes: gene duplication and loss define diverse ways to construct insect circadian clocks. *Mol. Biol. Evol.* **24**, 948–955. (doi:10.1093/molbev/msm011)
8. Partch CL, Green CB, Takahashi JS. 2014 Molecular architecture of the mammalian circadian clock. *Trends Cell Biol.* **24**, 90–99. (doi:10.1016/j.tcb.2013.07.002)
9. Cermakian N, Sassone-Corsi P. 2000 Multilevel regulation of the circadian clock. *Nat. Rev. Mol. Cell Biol.* **1**, 59–67. (doi:10.1038/35036078)
10. Dunlap JC. 1999 Molecular bases for circadian clocks. *Cell* **96**, 271–290. (doi:10.1016/s0092-8674(00)80566-8)
11. Box GEP, Jenkins GM, Reinsel GC. 1994 *Time series analysis: forecasting and control*, 3rd edn. Englewood Cliffs, NJ: Prentice Hall. See http://www.gbv.de/dms/bowker/toc/9780130607744.pdf.
12. Herrero MJ, Lepesant JMJ. 2014 Daily and seasonal expression of clock genes in the pituitary of the European sea bass (*Dicentrarchus labrax*). *Gen. Comp. Endocrinol.* **208**, 30–38. (doi:10.1016/j.ygcen.2014.08.002)
13. Goto SG. 2013 Roles of circadian clock genes in insect photoperiodism. *Entomol. Sci.* **16**, 1–16. (doi:10.1111/ens.12000)
14. Naylor E. 2010 *Chronobiology of marine organisms*. Cambridge, UK: Cambridge University Press. (doi:10.1017/cbo9780511803567)
15. Palmer JD. 1995 Review of the dual-clock control of tidal rhythms and the hypothesis that the same clock governs both circatidal and circadian rhythms. *Chronobiol. Int.* **12**, 299–310. (doi:10.3109/07420529509057279)
16. Perrigault M, Tran D. 2017 Identification of the molecular clockwork of the oyster *Crassostrea gigas*. *PLoS One* **12**, e0169790. (doi:10.1371/journal.pone.0169790)
17. Tran D, Perrigault M, Ciret P, Payton L. 2020 Bivalve mollusc circadian clock genes can run at tidal frequency. *Proc. R. Soc. B* **287**, 20192440. (doi:10.1098/rspb.2019.2440)
18. Chapman EC, O'Dell AR, Meligi NM, Parsons DR, Rotchell JM. 2017 Seasonal expression patterns of clock-associated genes in the blue mussel *Mytilus edulis*. *Chronobiol. Int.* **34**, 1300–1314. (doi:10.1080/07420528.2017.1363224)
19. Perrigault M, Andrade H, Bellec L, Ballantine C, Camus L, Tran D. 2020 Rhythms during the polar night: evidence of clock-gene oscillations in the Arctic scallop *Chlamys islandica*. *Proc. R. Soc. B* **287**, 20201001. (doi:10.1098/rspb.2020.1001)
20. Pogoda B. 2019 Current status of European oyster decline and restoration in Germany. *Humanities* **8**, 9. (doi:10.3390/h8010009)
21. zu Ermgassen PSE *et al*. 2020 The benefits of bivalve reef restoration: a global synthesis of underrepresented species. *Aquat. Conserv.* **30**, 2050–2065. (doi:10.1002/aqc.3410)
22. Pouvreau S, Lapègue S, Arzul I, Boudry P. 2023 Fifty years of research to counter the decline of the European flat oyster (*Ostrea edulis*): a review of French achievements and prospects for the restoration of remaining beds and revival of aquaculture production. *Aquat. Living Resour.* **36**, 13. (doi:10.1051/alr/2023006)
23. Pogoda B *et al*. 2020 Site selection for biogenic reef restoration in offshore environments: the Natura 2000 area Borkum Reef Ground as a case study for native oyster restoration. *Aquat. Conserv.* **30**, 2163–2179. (doi:10.1002/aqc.3405)
24. Colsoul B *et al*. 2021 Sustainable large-scale production of European flat oyster (*Ostrea edulis*) seed for ecological restoration and aquaculture: a review. *Rev. Aquac.* **13**, 1423–1468. (doi:10.1111/raq.12529)
25. Haelters J, Kerckhof F. 2009 Background document for *Ostrea edulis* and *Ostrea edulis* beds. OSPAR Biodiversity Series Publication, no. 428.
26. Pogoda B, Brown J, Hancock B, Preston J, Pouvreau S, Kamermans P, Sanderson W, von Nordheim H. 2019 The Native Oyster Restoration Alliance (NORA) and the Berlin oyster recommendation: bringing back a key ecosystem engineer by developing and supporting best practice in Europe. *Aquat. Living Resour.* **32**, 13. (doi:10.1051/alr/2019012)

27. Le Moal A, Tran D, Payton L, Pogoda B, Meyer B. 2025 Characterization of the daily and circadian valve behavior of the European flat oyster *Ostrea edulis*. *Sci. Rep.* **15**, 14952. (doi:10.1038/s41598-025-98746-x)
28. Davison A, Neiman M. 2021 Mobilizing molluscan models and genomes in biology. *Phil. Trans. R. Soc. B* **376**, 20200163. (doi:10.1098/rstb.2020.0163)
29. Adema CM. 2021 Sticky problems: extraction of nucleic acids from molluscs. *Phil. Trans. R. Soc. B* **376**, 20200162. (doi:10.1098/rstb.2020.0162)
30. Gundappa MK, Peñaloza C, Regan T, Boutet I, Tanguy A, Houston RD, Bean TP, Macqueen DJ. 2022 Chromosome-level reference genome for European flat oyster (*Ostrea edulis* L.). *Evol. Appl.* **15**, 1713–1729. (doi:10.1111/eva.13460)
31. Tran D, Andrade H, Camus L, Leopold P, Ballantine C, Berge J, Durier G, Sow M, Ciret P. 2023 Evidence of separate influence of moon and sun on light synchronization of mussel's daily rhythm during the polar night. *iScience* **26**, 106168. (doi:10.1016/j.isci.2023.106168)
32. Le Moal A, Payton L, Andrade H, Camus L, Ballantine C, Ciret P, Tran D. 2023 Blue mussels' valve behavior exhibits daily and lunar rhythms during the high Arctic polar day. *Mar. Biol.* **170**, 113. (doi:10.1007/s00227-023-04257-6)
33. Livak KJ, Schmittgen TD. 2001 Analysis of relative gene expression data using real-time quantitative PCR and the 2−ΔΔCT method. *Methods* **25**, 402–408. (doi:10.1006/meth.2001.1262)
34. Morga B, Arzul I, Faury N, Renault T. 2010 Identification of genes from flat oyster *Ostrea edulis* as suitable housekeeping genes for quantitative real time PCR. *Fish Shellfish Immunol.* **29**, 937–945. (doi:10.1016/j.fsi.2010.07.028)
35. Du Y, Zhang L, Xu F, Huang B, Zhang G, Li L. 2013 Validation of housekeeping genes as internal controls for studying gene expression during Pacific oyster (*Crassostrea gigas*) development by quantitative real-time PCR. *Fish Shellfish Immunol.* **34**, 939–945. (doi:10.1016/j.fsi.2012.12.007)
36. Vandesompele J, De Preter K, Pattyn F, Poppe B, Van Roy N, De Paepe A, Speleman F. 2002 Accurate normalization of real-time quantitative RT-PCR data by geometric averaging of multiple internal control genes. *Genome Biol.* **3**, h0034. (doi:10.1186/gb-2002-3-7-research0034)
37. Bustin SA *et al*. 2009 The MIQE guidelines: minimum information for publication of quantitative real-time PCR experiments. *Clin. Chem.* **55**, 611–622. (doi:10.1373/clinchem.2008.112797)
38. Scargle JD. 1982 Studies in astronomical time series analysis. II. Statistical aspects of spectral analysis of unevenly spaced data. *Astrophys. J.* **263**, 835. (doi:10.1086/160554)
39. Bingham C, Arbogast B, Guillaume GC, Lee JK, Halberg F. 1982 Inferential statistical methods for estimating and comparing cosinor parameters. *Chronobiologia* **9**, 397–439.
40. R Core Team. 2023 *R: a language and environment for statistical computing*. Vienna, Austria: R Foundation for Statistical Computing. See https://www.R-project.org/.
41. Thaben PF, Westermark PO. 2014 Detecting rhythms in time series with RAIN. *J. Biol. Rhythm.* **29**, 391–400. (doi:10.1177/0748730414553029)
42. Schmalen I, Reischl S, Wallach T, Klemz R, Grudziecki A, Prabu JR, Benda C, Kramer A, Wolf E. 2014 Interaction of circadian clock proteins CRY1 and PER2 is modulated by zinc binding and disulfide bond formation. *Cell* **157**, 1203–1215. (doi:10.1016/j.cell.2014.03.057)
43. Nangle SN, Rosensweig C, Koike N, Tei H, Takahashi JS, Green CB, Zheng N. 2014 Molecular assembly of the period-cryptochrome circadian transcriptional repressor complex. *eLife* **3**, e03674. (doi:10.7554/elife.03674)
44. Jetten AM, Joo JH. 2006 Retinoid-related orphan receptors (RORs): roles in cellular differentiation and development. *Adv. Develop. Biol.* **16**, 313–355. (doi:10.1016/S1574-3349(06)16010-X)
45. Nawathean P, Rosbash M. 2004 The doubletime and CKII kinases collaborate to potentiate *Drosophila* PER transcriptional repressor activity. *Mol. Cell* **13**, 213–223. (doi:10.1016/s1097-2765(03)00503-3)
46. Matsumoto A *et al*. 2007 A functional genomics strategy reveals *clockwork orange* as a transcriptional regulator in the *Drosophila* circadian clock. *Genes Dev.* **21**, 1687–1700. (doi:10.1101/gad.1552207)
47. Foulkes NS, Borjigin J, Snyder SH, Sassone-Corsi P. 1997 Rhythmic transcription: the molecular basis of circadian melatonin synthesis. *Trends Neurosci.* **20**, 487–492. (doi:10.1016/s0166-2236(97)01109-0)
48. Bellingham J, Whitmore D, Philp AR, Wells DJ, Foster RG. 2002 Zebrafish melanopsin: isolation, tissue localisation and phylogenetic position. *Mol. Brain Res.* **107**, 128–136. (doi:10.1016/s0169-328x(02)00454-0)
49. Peirson S, Foster RG. 2006 Melanopsin: another way of signaling light. *Neuron* **49**, 331–339. (doi:10.1016/j.neuron.2006.01.006)
50. Hankins MW, Peirson SN, Foster RG. 2008 Melanopsin: an exciting photopigment. *Trends Neurosci.* **31**, 27–36. (doi:10.1016/j.tins.2007.11.002)
51. Reppert SM, Weaver DR. 2002 Coordination of circadian timing in mammals. *Nature* **418**, 935–941. (doi:10.1038/nature00965)
52. Biscontin A *et al*. 2017 Functional characterization of the circadian clock in the Antarctic krill, *Euphausia superba*. *Sci. Rep.* **7**, 17742. (doi:10.1038/s41598-017-18009-2)
53. Zantke J, Ishikawa-Fujiwara T, Arboleda E, Lohs C, Schipany K, Hallay N, Straw AD, Todo T, Tessmar-Raible K. 2013 Circadian and circalunar clock interactions in a marine annelid. *Cell Rep.* **5**, 99–113. (doi:10.1016/j.celrep.2013.08.031)
54. Stanton D, Justin HS, Reitzel AM. 2022 Step in time: conservation of circadian clock genes in animal evolution. *Integr. Comp. Biol.* **62**, 1503–1518. (doi:10.1093/icb/icac140)
55. Guillaumond F, Dardente H, Giguère V, Cermakian N. 2005 Differential control of Bmal1 circadian transcription by REV-ERB and ROR nuclear receptors. *J. Biol. Rhythm.* **20**, 391–403. (doi:10.1177/0748730405277232)
56. Relógio A, Westermark PO, Wallach T, Schellenberg K, Kramer A, Herzel H. 2011 Tuning the mammalian circadian clock: robust synergy of two loops. *PLoS Comput. Biol.* **7**, e1002309. (doi:10.1371/journal.pcbi.1002309)

57. Zeng Z, Ni J, Ke C. 2013 Expression of glycogen synthase (GYS) and glycogen synthase kinase 3β (GSK3β) of the Fujian oyster, *Crassostrea angulata*, in relation to glycogen content in gonad development. *Comp. Biochem. Physiol. B* **166**, 203–214. (doi:10.1016/j.cbpb.2013.09.003)
58. Hüppe L, Payton L, Last K, Wilcockson D, Ershova E, Meyer B. 2020 Evidence for oscillating circadian clock genes in the copepod *Calanus finmarchicus* during the summer solstice in the high Arctic. *Biol. Lett.* **16**, 20200257. (doi:10.1098/rsbl.2020.0257)
59. Sun XJ, Zhou LQ, Tian JT, Liu ZH, Wu B, Dong YH, Yang AG, Ma WM. 2016 Transcriptome survey of phototransduction and clock genes in marine bivalves. *Genet. Mol. Res.* **15**, 1–10. (doi:10.4238/gmr15048726)
60. Öztürk N, Song SH, Özgür S, Selby CP, Morrison L, Partch C, Zhong D, Sancar A. 2007 Structure and function of animal cryptochromes. *Cold Spring Harb. Symp. Quant. Biol.* **72**, 119–131. (doi:10.1101/sqb.2007.72.015)
61. Chaves I *et al*. 2011 The cryptochromes: blue light photoreceptors in plants and animals. *Annu. Rev. Plant Biol.* **62**, 335–364. (doi:10.1146/annurev-arplant-042110-103759)
62. Peschel N, Chen KF, Szabo G, Stanewsky R. 2009 Light-dependent interactions between the *Drosophila* circadian clock factors cryptochrome, jetlag, and timeless. *Curr. Biol.* **19**, 241–247. (doi:10.1016/j.cub.2008.12.042)
63. Emery P, So WV, Kaneko M, Hall JC, Rosbash M. 1998 CRY, a *Drosophila* clock and light-regulated cryptochrome, is a major contributor to circadian rhythm resetting and photosensitivity. *Cell* **95**, 669–679. (doi:10.1016/s0092-8674(00)81637-2)
64. Emery P, Stanewsky R, Helfrich-Förster C, Emery-Le M, Hall JC, Rosbash M. 2000 *Drosophila* CRY is a deep brain circadian photoreceptor. *Neuron* **26**, 493–504. (doi:10.1016/s0896-6273(00)81181-2)
65. Lin FJ, Song W, Meyer-Bernstein E, Naidoo N, Sehgal A. 2001 Photic signaling by cryptochrome in the *Drosophila* circadian system. *Mol. Cell. Biol.* **21**, 7287–7294. (doi:10.1128/mcb.21.21.7287-7294.2001)
66. Stanewsky R, Kaneko M, Emery P, Beretta B, Wager-Smith K, Kay SA, Rosbash M, Hall JC. 1998 The cryb mutation identifies cryptochrome as a circadian photoreceptor in *Drosophila*. *Cell* **95**, 681–692. (doi:10.1016/s0092-8674(00)81638-4)
67. Zhu H, Yuan Q, Froy O, Casselman A, Reppert SM. 2005 The two CRYs of the butterfly. *Curr. Biol.* **15**, R953–R954. (doi:10.1016/j.cub.2005.11.030)
68. Christie AE, Fontanilla TM, Nesbit KT, Lenz PH. 2013 Prediction of the protein components of a putative *Calanus finmarchicus* (Crustacea, Copepoda) circadian signaling system using a de novo assembled transcriptome. *Comp. Biochem. Physiol. D* **8**, 165–193. (doi:10.1016/j.cbd.2013.04.002)
69. Häfker NS, Meyer B, Last KS, Pond DW, Hüppe L, Teschke M. 2017 Circadian clock involvement in zooplankton diel vertical migration. *Curr. Biol.* **27**, 2194–2201.(doi:10.1016/j.cub.2017.06.025)
70. Zhang M *et al*. 2023 Effects of light on growth, feeding rate, digestion, and antioxidation in juvenile razor clams *Sinonovacula constricta*. *Aquaculture* **568**, 739306. (doi:10.1016/j.aquaculture.2023.739306)
71. Botte A, Payton L, Tran D. 2023 The effects of artificial light at night on behavioral rhythm and related gene expression are wavelength dependent in the oyster *Crassostrea gigas*. *Environ. Sci. Pollut. Res.* **30**, 120375–120386. (doi:10.1007/s11356-023-30793-1)
72. Ikegami K, Yoshimura T. 2017 Molecular mechanism regulating seasonality. In *Biological timekeeping: clocks, rhythms and behaviour* (ed. V Kumar), pp. 589–605. New Delhi, India: Springer. (doi:10.1007/978-81-322-3688-7_28)
73. Reiter RJ. 1993 The melatonin rhythm: both a clock and a calendar. *Experientia* **49**, 654–664. (doi:10.1007/bf01923947)
74. Tosches MA, Bucher D, Vopalensky P, Arendt D. 2014 Melatonin signaling controls circadian swimming behavior in marine zooplankton. *Cell* **159**, 46–57. (doi:10.1016/j.cell.2014.07.042)
75. Fabra M, Morrall Z, Helmer L, Watson G, Preston J. 2024 Filtration behaviour of *Ostrea edulis*: diurnal rhythmicity influenced by light cycles, body size and water temperature. *Estuaries Coast.* **48**, 18. (doi:10.1007/s12237-024-01453-5)
76. Mure LS *et al*. 2018 Diurnal transcriptome atlas of a primate across major neural and peripheral tissues. *Science* **359**, o0318. (doi:10.1126/science.aao0318)
77. Enright JT. 1976 Plasticity in an isopod's clockworks: shaking shapes form and affects phase and frequency. *J. Comp. Physiol.* **107**, 13–37. (doi:10.1007/bf00663916)
78. Mat AM, Perrigault M, Massabuau JC, Tran D. 2016 Role and expression of cry1 in the adductor muscle of the oyster *Crassostrea gigas* during daily and tidal valve activity rhythms. *Chronobiol. Int.* **33**, 949–963. (doi:10.1080/07420528.2016.1181645)
79. Payton L *et al*. 2017 Remodeling of the cycling transcriptome of the oyster *Crassostrea gigas* by the harmful algae *Alexandrium minutum*. *Sci. Rep.* **7**, 3480. (doi:10.1038/s41598-017-03797-4)
80. Le Moal A *et al*. 2025 . Supplementary material from: Identification and expression of circadian clock genes in the European flat oyster *Ostrea edulis*. Figshare. (doi:10.6084/m9.figshare.c.8154231)